Experimental Comparison of Motor Bearing Currents with PWM Hard and Soft Switched Voltage Source Inverters

S. Bhattacharya * L. Resta + D. M. Divan * D. W. Novotny * T. A. Lipo *

* Department of Electrical and Computer Engineering
University of Wisconsin-Madison
1415 Johnson Drive, Madison, WI 53706, USA
Tel:608-265-3815/608-262-5702/608-262-6926/608-262-0287/Fax:608-262-1267
Email:bhattach@cae.wisc.edu/divan@engr.wisc.edu/novotny@engr.wisc.edu/lipo@engr.wisc.edu
+ SIEI Peterlongo, ITALY

Abstract— **This paper compares motor bearing currents due to PWM hard switched and soft switched inverters. The mechanisms for bearing currents are first identified using an approach based on direct excitation of the motor bearing with sinusoidal and square-wave signals to characterize the bearings. It is shown that many of the motor models that have been proposed in the literature to explain bearing currents do not adequately explain the observed higher frequency effects. The paper also outlines some of the important phenomena which need to be considered for a more complete description of bearing currents. Finally, the paper compares the performance of hard and soft switched inverters with respect to bearing currents. Experimental results are provided for PWM hard switched and soft switched IGBT inverters which have exactly same power circuit layout, identical chassis and rating of 70 kW.**

I. Introduction

The motor and drives industry has, yet again, focused its attention on the problem of drive related motor failures. The problem of dv/dt related winding insulation failures is generally understood, and occurs due to uneven distribution of voltage stresses along a distributed winding, which can be greatly increased by standing waves along long cables between the inverter and the drive. Both phenomena relate to the very high frequency content in the inverter switching waveform, and understanding it requires that an appropriate high frequency model of the motor and cable be used. The problem is remedied in industry by the use of dv/dt limiting networks or, more recently, by the use of zero voltage switching soft switching inverters. However, use of differential or common mode reactors may not solve, and may actually exacerbate, the problem.

The second important motor failure mechanism receiving attention of late is that of motor bearing failures. Bearing failures occur due to currents flowing through the bearings, which cause pitting and fluting of the bearing races, and of the balls in the bearings. Motor reliability studies indicate that motor bearing failures are the primary cause of motor failures and account for 40% of the total failures [1],[2]. The issue of shaft voltages, bearing currents and related bearing failures in motors under *sinusoidal excitation* has been known for many years [3]. Early concerns were primarily linked to electromagnetic induction resulting from asymmetries in the air gap magnetic field. Bearing failures have also been reported for large turbogenerators with thyristor based static excitation systems [4]. Improvements in machine design and bearings has brought these problems under control. Every time there has been a change in the technology base for adjustable speed ac drives, there has been a resurgence of concern about bearing (and winding) failures. With the introduction of IGBT based inverters, bearing failures have again increased causing concern to motor and drive manufacturers, as well as to users. This concern was reflected at the recent EASA (Electrical Apparatus Service Association) Convention in Phoenix (USA) in February 1996, where a large part of the conference was devoted to the issues of winding and bearing failures. Bearing manufacturers represented that almost 25% of all bearing failures were due to dv/dt, and that this number was increasing quite dramatically [5]. A recent spate of papers on bearing and winding failures from some of the most reputed motor and drive manufacturers also suggests that this problem is very real [6] [15].

This paper reexamines the issue of bearing currents. While identifying the root cause of bearing failures may be difficult, an understanding of the various mechanisms causing bearing current flow is very important. Once all the basic mechanisms are understood, and correlate well with field failure data, a model which can be reasonably applied to identifying the root cause of the failures may be possible. A step in this direction was taken by an approach based on direct excitation of the bearing with sinusoidal and square-wave excitations to isolate various bearing current components. A final important test relates to the use of identical hard and soft switching inverters and the level of bearing currents flowing in both cases.

II. Motor Equivalent Circuit Revisited

Much of the past analysis of motor bearing currents is based upon the intermediate frequency machine model shown in figure 1 and its common mode equivalent circuit model shown in figure 2. Previous work [7]-[10],[14]-[16] has suggested that the capacitance between the stator winding and the stator iron can be represented in a lumped form. Further, the capacitance between the windings and the rotor is also assumed to be lumped. It is assumed that *electrostatically* induced shaft voltages due to PWM inverters cause the charging of the bearing capacitance C_{sr}. The bearing itself is modeled with a randomly shorting contact in series with a non-linear resistance R_s, as shown in figure 2, which causes a discharge of the bearing capacitance, resulting in large current spikes. These current spikes have been referred to as causing 'electric discharge machining' (EDM), with the implication that they represent the culprit for bearing damage [7]-[10],[14],[15]. The authors suggest in this paper that the overall situation is more complex than this.

It is instructive to further analyze the cause and effect relationship between the various voltages and the bearing currents observed. The various components of bearing current that need to be explained include EDM components, dv/dt related components, and any other sources that could result in the offending current. Examining the dv/dt related current, it is clear that the inverter voltages, particularly for hard switched inverters, have rise times of 0.1 μs and associated frequency components of the order of $10 - 30$ MHz. This suggests that any motor model one uses to examine currents generated during the switching transient should be valid over that range of frequencies. This is not as unusual as one might think, as the impact of dv/dt on winding

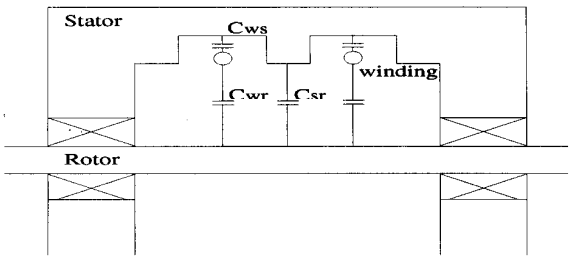

Fig. 1. Intermediate frequency lumped parameter induction motor model

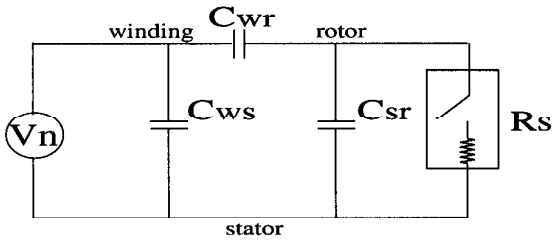

Fig. 2. Intermediate frequency common mode equivalent circuit

insulation stresses requires a similar analysis.

The motor model is symmetric at low frequencies, as can be judged by the *neutral voltage* behavior under sinusoidal excitation. Figure 3 shows a typical neutral voltage under PWM inverter excitation [15], which has been referred to as the *'common mode voltage' seen by the motor* [7],[14],[15]. The neutral voltage waveform is seen to have low dv/dt at the edges, representing relatively low frequency content, suggesting that the cause of both the shaft voltage and bearing current is the inverter dv/dt and resulting high frequency common mode voltage.

What is important at this point is to examine what the model of the motor may be in the high frequency range of $10 - 30$ MHz identified above. It seems clear that at least at frequencies below 50 kHz, the low frequency model may be sufficient to describe bearing current behavior. At higher frequencies, it has been shown [17]-[19] that the motor model is highly unpredictable and asymmetric, not only from machine to machine, but also from winding to winding within the same machine. A simplified asymmetrical high frequency induction motor model is shown in figure 4. Note that at high frequencies the capacitive and inductive couplings of each phase are different depending on the spatial asymmetry of the winding to the shaft and bearings, as indicated by unequal coupling capacitors C_1, C_2 and C_3. The low frequency capacitive coupling to the motor neutral has been omitted in figure 4 for simplicity. The asymmetric nature of the motor model at high frequencies is understandable, because the high frequency capacitively coupled currents depend strongly on the location of the first few turns within the slot, a parameter which is not well controlled in random wound machines by any motor manufacturer. Capacitive currents are coupled locally to the stator iron, and then flow as dictated by potentials and impedances within the iron. A second factor which

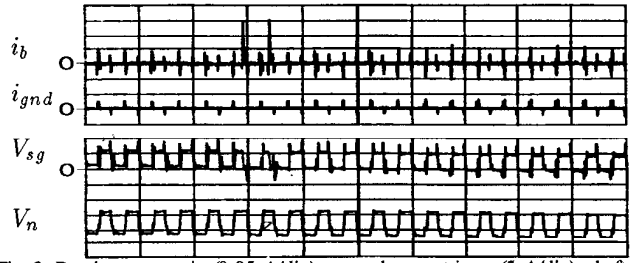

Fig. 3. Bearing current i_b (0.05 A/div), ground current i_{gnd} (5 A/div), shaft voltage V_{sg} [5 V/div], neutral voltage V_n [100 V/div], $t = 200\mu s$/div

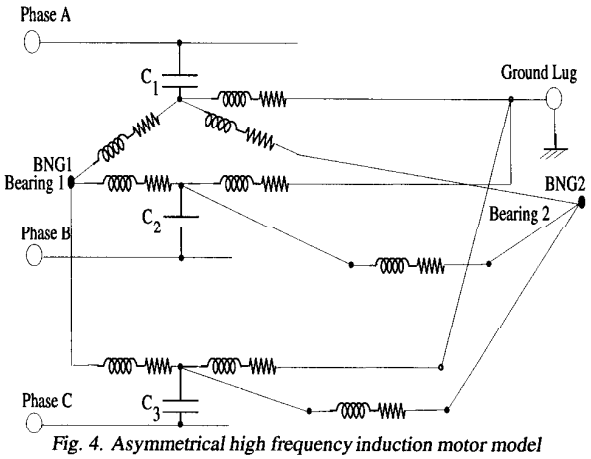

Fig. 4. Asymmetrical high frequency induction motor model

adds substantially to this asymmetry is the path taken by these coupled capacitive currents. Every inverter switching event can be considered to be a local phenomenon in specific parts of the motor winding and stator. It is also observed that high frequency currents are coupled into the stator iron when the neutral voltage is unchanged, which suggests the presence of *'high frequency common mode voltage'* signal due to asymmetric nature of the machine at high frequencies. The stator iron with its finite high frequency impedance and the local capacitances from the excited windings to its 'local' iron will govern the amplitude and distribution of the capacitively coupled current that flows in the stator iron. In fact a substantial part of this current actually flows into the motor frame grounding lug, resulting in the ground currents that can easily be observed in any inverter drive. It is interesting to note that the grounding lug is typically a single point connection, and depending on the location of its connection to the stator iron, can further contribute to the high frequency asymmetry of the machine.

III. Shaft Voltages from Low Frequency Common Mode Voltages

The above discussion implies that at least two phenomena contribute to shaft voltages observed in induction machines. The first phenomenon is based on the low frequency model of the machine, and is coupled through the various capacitances identified in figure 2. The resulting neutral voltage contributes an effective voltage across the bearing capacitance when the bearing is in its non-conductive state. This voltage has been observed and identified by virtually all the papers discussing the issue of inverter related bearing currents. The 'bearing voltage' is related to the inverter common mode voltage, as is suggested by the low frequency model, and has been verified by several authors including [15]. Experimental observations and simulations have verified that this voltage can be as high as $10 - 20$ V. It is well known that a substantial current pulse of as much as 0.5 to 3 Amperes peak flows in the bearing when the bearing lubricant film breaks down. The high current flowing under these conditions is the previously described EDM current which has been suggested as the primary cause for bearing degradation [7]-[10],[14],[15].

It is clear that the EDM current has a high peak value, and as such is capable of significant damage at the bearing surface. There are two reasons for this current to flow. The first is due to random mechanical contact as one of the balls pierces the lubricant film and makes contact with the race. This seems to happen more frequently at lower motor speeds, and less often as motor speed increases. In any case, the random contact occurs at a frequency much lower than the inverter

switching frequency. When it does occur, the bearing capacitance is discharged resulting in the large current pulses described above. If this is the dominant mode of bearing damage, we are left with the question of why bearing failure rates have reportedly increased dramatically with the advent of IGBT inverters. These peak intermediate frequency neutral voltages, and thus the dependent bearing voltages, are independent of dv/dt or frequency of switching, and should be similar for both BJT and IGBT inverters. Since different rates of failure are observed in these two types of inverters, the effect on the bearing of the EDM currents is not likely the only contributor to bearing failure.

The second reason for current flow is that the field strength at the peak of the bearing voltage is sufficient to break down the insulation level of the lubricant film. However, this is not in agreement with the fact that EDM currents do not flow at every pulse, but only at infrequent intervals.

IV. Shaft Voltages Resulting From Motor Asymmetries

The second phenomenon contributing to shaft voltage is related to high frequency dv/dt induced currents. It has been pointed out that the high dv/dt of the inverter waveform is absorbed asymmetrically in relation to the spatial characteristics of the motor. Further, the steep edge of the voltage is absorbed in conformance with stator iron impedances related to the geometric construction of the motor. Another important issue is the high frequency common mode current that is coupled to the motor ground. In classical low frequency terms, there should be no induced ground currents in the case where, for instance, two inverter phases change polarity leaving the neutral voltage unaltered. Note that the neutral voltage is unchanged if two inverter switches simultaneously change state or equivalently for transitions between either odd to odd or even to even active inverter states. This is not seen to be the case, and there is a spike of dv/dt related current which flows in the ground lead. As a high frequency pulse of current flows in the stator iron inductance and resistance, it can induce a voltage between the two bearing points, showing up as a shaft voltage. This voltage will clearly have a dominant component related to the dv/dt. At lower frequencies where the model of figure 2 is valid, this voltage is effectively zero. This implies that the spatial asymmetries of the motor windings, core and ground can create a voltage across the bearing lubricant film. This also raises the interesting point that dv/dt induced shaft voltages may have a conductive dependence, and the possibility that the shaft voltages may be highest for low impedance connections between the machine case and system ground. The final analysis of conductively induced shaft voltages would depend on the machine design and on system connection impedances. This conductively induced shaft voltage is in addition to asymmetrically flux induced shaft voltages.

The characteristic of this voltage is a significant level of high frequency content, as it is generated by the flow of dv/dt induced currents in predominantly inductive impedance paths in the stator iron. While the behavior of the bearing lubricant film under steady state voltage is well known, there is little experimental data on its properties under high frequency excitation.

The above discussion shows the difficulty in implementation of a *single* machine model for simulation of bearing current components. Further, the high frequency model requires characterization of various capacitances and inductances as a function of frequency by extensive measurements. Alternatively, a simple model based on lumped parameters does not predict all bearing current components [7]-[10],[14],[15].

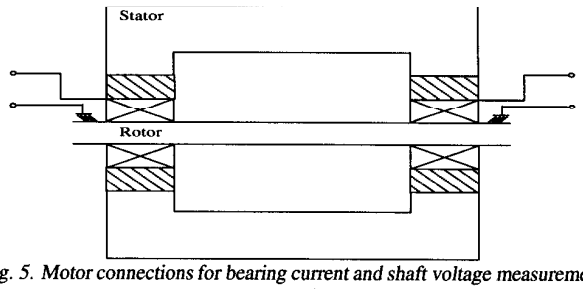

Fig. 5. Motor connections for bearing current and shaft voltage measurement

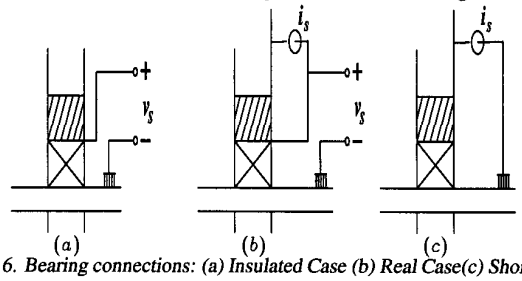

Fig. 6. Bearing connections: (a) Insulated Case (b) Real Case(c) Shorted Case

V. Bearing Behavior Under Direct Excitation

The difficulty of measuring relevant data in a high noise (i.e. dv/dt) environment is well known. Oscilloscope measurements of small bearing voltages when PWM inverters are switching at 10,000 volts per microsecond are difficult. Measurement of bearing behavior under 'direct excitation', when the motor was rotated externally with its terminals shorted, was attempted to provide a sensitive noise free environment for characterizing the bearing itself.

A special 10 hp, 4 pole, 3 phase, 460 V induction motor was supplied by MagneTek for this test. The bearings of the motor were insulated, but were accessible electrically using wires which were connected to the bearing outer races. A brush was also connected to the shaft on either end of the motor as shown in figure 5. Connecting the wires to the motor housing was equivalent to operating this machine normally. However, by inserting a current probe in the above wire, it was possible to measure the currents flowing in the bearing. One could also connect the bearing outer race to the shaft via the brush, effectively shorting the bearing allowing measurements of current in a shorted bearing. These three connections are shown in figure 6(a,b,c).

Capacitive coupling measurements by a QuadTech 7400 impedance analyser at 100 kHz for the MagneTek 10 hp motor are given below:

$C_{ws} = 5\,nF \qquad C_{wr} = 10\,pF \qquad C_{sr} = 920\,pF$

The motor was driven by a variable speed dc motor, and was instrumented with voltage and current probes. The parameters of the experiment are shaft speed, amplitude, frequency and waveform type of the exciting signal. Low frequency 60 Hz sinusoidal excitation was first applied across the normal bearing to observe bearing currents. At low rotational speeds the bearings tend to conduct most of the time. As the speed increased to a few hundred rpm, the lubricant film became essentially insulating, and the only current observed was due to random mechanical shorting of the bearing. This resulted in high peak currents, as shown in figure 7 with 100 kHz sinusoidal excitation of 1 V peak-peak and shaft speed of 500 rpm, and corresponds to the phenomenon which has been referred to as EDM current [7]. As the applied voltage is increased, the bearing tends to lose its insulating properties more frequently, as seen in figure 8, and can initiate an EDM discharge as the voltage reaches a peak. This phenomenon seems to be related to lubricant film dielectric breakdown, and has been reported previously.

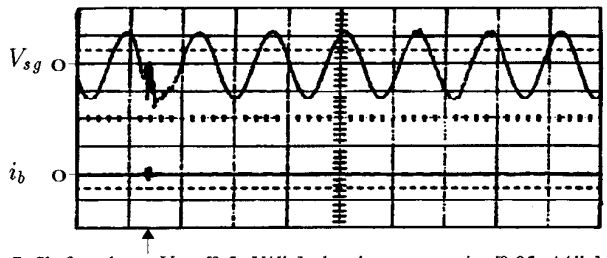

Fig. 7. Shaft voltage V_{sg} [0.5 V/div], bearing current i_b [0.05 A/div], t = 5μs/div ; sinusoidal excitation voltage showing EDM current spike by arrow

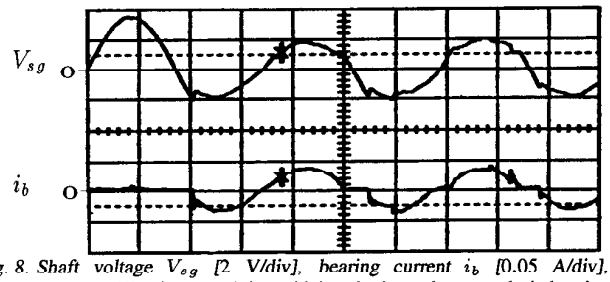

Fig. 8. Shaft voltage V_{sg} [2 V/div], bearing current i_b [0.05 A/div]. t = 5μs/div ; increased sinusoidal excitation voltage results in bearing breakdown and continuous bearing current

The breakdown voltage under the above conditions was measured to be in the range of 8 – 20 V peak-peak at 500 rpm. It was interesting to note that as the driving voltage of the excitation was increased to well above the point at which breakdown was initiated, the bearing did not immediately recover its blocking property and continued to continuously conduct current, even through the zero crossings of the excitation voltage, as shown in figure 9. This seems to indicate that with high current flow through the film, sufficient ionization occurs to make the bearing conductive for a significant period of time. It is also important to note that as the voltage across the bearing seldom built up, the EDM mode of high current discharge occurred infrequently as explained before, and also had much lower peak amplitude.

As the frequency of the excitation voltage was increased, the peak voltage at which bearing breakdown occurred reduced significantly. This suggested a strong frequency dependence on the lubricant film breakdown behavior. Experiments with sinusoidal excitation simulate soft switching inverter conditions. The tests showed similar results when the excitation voltage was a low frequency triangular waveform.

Experiments with square-wave excitation simulate PWM hard switched inverter conditions. The results under square wave excitation, particularly at higher frequencies (100 kHz) showed that the film voltage sustaining capability was reduced to as low as 1 – 2 V at a shaft speed of 500 rpm, as shown in figure 10. the applied square

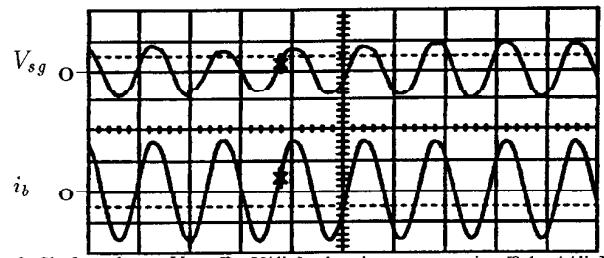

Fig. 9. Shaft voltage V_{sg} [2 V/div], bearing current i_b [0.1 A/div], t = 5μs/div ; continuous bearing current through zero crossings of sinusoidal excitation voltage

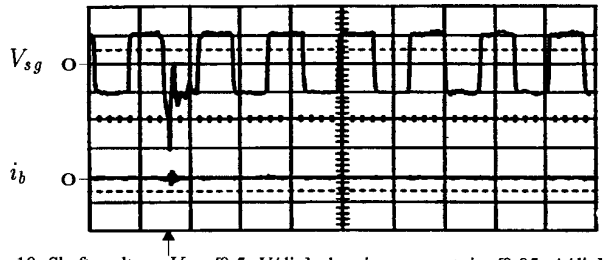

Fig. 10. Shaft voltage V_{sg} [0.5 V/div], bearing current i_b [0.05 A/div], t = 5μs/div ; square-wave excitation voltage showing EDM current spike by arrow

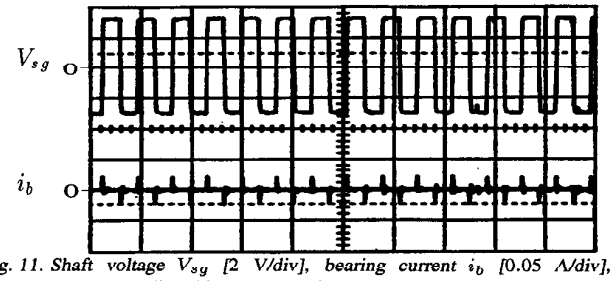

Fig. 11. Shaft voltage V_{sg} [2 V/div], bearing current i_b [0.05 A/div], t = 5μs/div ; higher dv/dt of square-wave excitation voltage results in dv/dt induced bearing current

wave voltage with lubricant breakdown, with higher dv/dt resulting in earlier breakdown of the lubricant film. This is illustrated in figure 11 with 6 V peak-peak square-wave excitation at 100 kHz at a shaft speed of 500 rpm producing bearing current at each voltage transition. The bearings also show occasional periods of continuous conduction once breakdown was initiated at the voltage transition point, as shown in figure 12, under the same conditions as that in figure 11. It can also be seen from figure 11 and figure 12 that the most striking feature of this dv/dt induced bearing current is the presence of a current spike which does not change much with frequency unless the dv/dt is also changed. This suggests that the effective bearing capacitance causes the current flow in response to the dv/dt. It should be noted however, that in the presence of high dv/dt, the shaft voltage did not reach the levels possible under sinusoidal excitation, indicating much higher susceptibility to field induced voltage breakdown. Finally, although there is a dv/dt related current spike in the bearing, it does not seem to be solely as a consequence of the low frequency capacitive model of the induction machine.

The authors propose that the shaft voltage occurring across the bearings is also due to high frequency machine effects, and that this voltage has substantial high frequency content which tends to accelerate breakdown of the bearing lubricant film. The presence of this

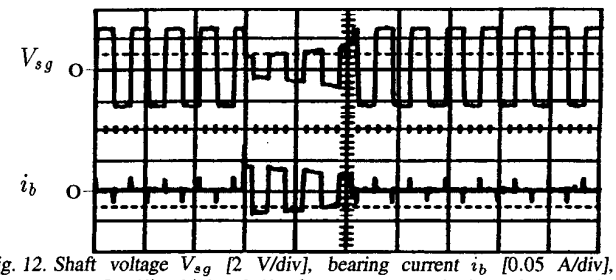

Fig. 12. Shaft voltage V_{sg} [2 V/div], bearing current i_b [0.05 A/div], t = 5μs/div ; higher dv/dt of square-wave excitation voltage results in bearing breakdown with continuous conduction and dv/dt induced bearing current

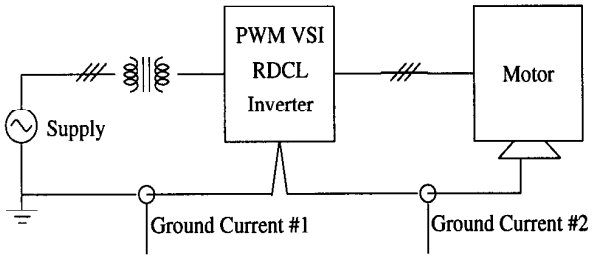

Fig. 13. Experimental set-up for comparison of motor bearing currents with PWM inverter and resonant dc link (RDCL) soft switched inverter

driving voltage will be verified in the next section.

Several important issues have been brought to the forefront as a result of the direct excitation experiment. Firstly, it highlights the role played by dv/dt in bearing currents, and in the voltage sustaining capability of the lubricant film. Spike currents due to dv/dt have been observed by previous authors [7][8], but have been discarded as a possible contributor to accelerated bearing failure. In addition to causing bearing damage through material removal (EDM), it seems likely that the spike current causes local ionization in the lubricant film which further reduces the voltage sustain capability. It also indicates the possibility of a hitherto unreported phenomenon, in that under higher voltage excitation, the bearing tends to remain conducting for a while even after the voltage is reduced, increasing the rms current flow in the bearing. Finally, the experiments support the suggestion that the current flowing due to random mechanical contact is not the only factor relating to bearing failure mechanism. The next stage in the process was to drive the same machine with an identically rated hard switched PWM inverter and a soft switched resonant dc link inverter.

VI. Experimental Comparison With Inverter Driven Motor

A special 15 hp, 8 pole, 3 phase, 460 V induction motor was supplied by Marathon Electric Co. for this test and was driven by two inverters, each rated at 70 kVA, 460 V. The hard switched PWM inverter is a commercially available unit with a switching frequency of 7 kHz. The soft switched resonant dc link (RDCL) inverter was built using the same cabinet, heatsink, dc capacitors and power circuit layout. The actively clamped resonant dc link circuit operated with a resonant link frequency of 65 kHz with a sigma-delta voltage modulator, which has higher common mode voltage compared to other improved sigma-delta modulators [20],[21]. The modulator and inductor were not designed for low common mode voltage, and are seen to be worse than are possible with newer designs. The measurement of bearing currents in the presence of inverter switching noise is difficult, and care was taken to follow consistent grounding procedures. The experimental set-up is shown in figure 13.

Capacitive coupling measurements by a QuadTech 7400 impedance analyser at 100 kHz for the Marathon 15 hp motor are given below. The capacitive couplings are higher compared to the 10 hp motor due to larger size.

$C_{ws} = 11\ nF \qquad C_{wr} = 80\ pF \qquad C_{sr} = 1200\ pF$

The motor was operated with its bearings in various modes, corresponding to *insulated, real* and *shorted* modes for each bearing. The more useful configurations included; *insulated-real, insulated-shorted, real-real, real-shorted, and shorted-shorted.* The *insulated-real* case allows measurement of shaft voltage at the insulated end, and current at the real end. The *insulated-shorted* case does not permit the EDM mode of discharge current, and shows the level of current flowing if the lubricant breaks down. The *real-real* case provides a real life scenario of currents that may flow in the bearings. The *real-shorted* case demonstrates the level of current flow that could occur if one bearing became damaged. Finally, the *shorted-shorted* case shows current flow that occurs as both bearings become progressively damaged.

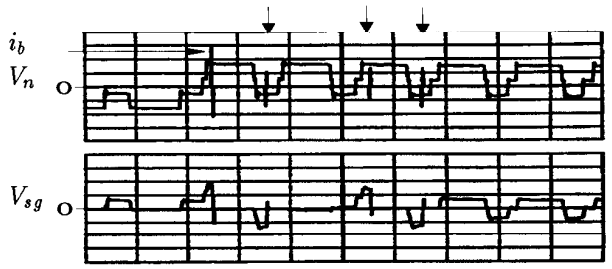

Fig. 14. Insulated-Real case with PWM inverter ; bearing current i_b [1 A/div], neutral voltage V_n [200 V/div], shaft voltage V_{sg} [20 V/div], $t = 100\mu s/div$; arrows indicate bearing current spikes

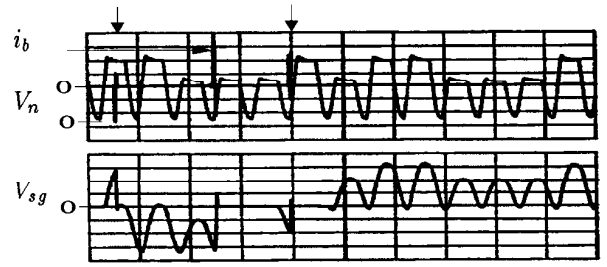

Fig. 15. Insulated-Real case with RDCL inverter ; bearing current i_b [1 A/div], neutral voltage V_n [200 V/div], shaft voltage V_{sg} [20 V/div], $t = 20\mu s/div$; arrows indicate bearing current spikes

Figures 14 and 15 show the *insulated-real* case for PWM hard switched and soft switched resonant dc link inverter types respectively, demonstrating random discharge mode currents. The shaft voltages are higher for the resonant dc link inverter due to poor common mode design, and give higher peak currents (4 A versus 3 A) when discharge occurs. However, breakdown in both cases is very infrequent. Expanding the current waveform shows that the PWM hard switched inverter case also has current spikes of 0.05 – 0.3 A peak corresponding to each inverter switching instant. This current is independent of whether the bearing is sustaining voltage or is conducting as shown in figure 16. Figure 16 shows evidence of conductively induced shaft voltage as explained in section IV. Bearing current spike is observed in figure 16 in the presence of conductively induced shaft voltage and when the neutral voltage is constant. For the resonant dc link, there is seen to be virtually no current when the bearing is normal, and some small current when the bearing is conductive following a discharge, as shown in figure 17. The above result is further confirmed by observing the *insulated-shorted* case, which gave similar results, as shown in figures 18 and 19 for PWM hard switched and soft switched resonant dc link inverter types respectively. This case constrains the shaft voltage to zero and avoids discharge mode bearing current. It should be noted that the *insulated-shorted* case also demonstrates the existence of voltage spikes on the shaft voltage, corresponding to the flow of high frequency dv/dt induced currents as discussed in section IV.

In the *real-real* case, shown in figures 20 and 21, it is seen that dv/dt related currents are the dominant current component, with infrequent additional spikes due to discharge mode as expected. In the resonant

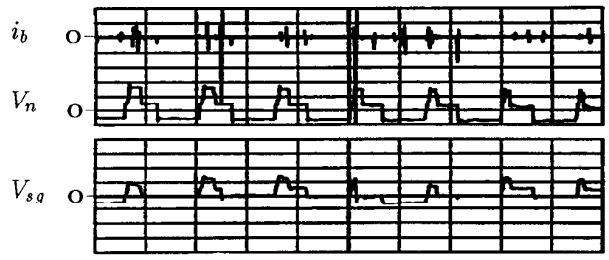

Fig. 16. Insulated-Real case with PWM inverter; bearing current i_b [0.1 A/div] expanded scale, neutral voltage V_n [200 V/div], shaft voltage V_{sg} [20 V/div], $t = 100\mu s$/div

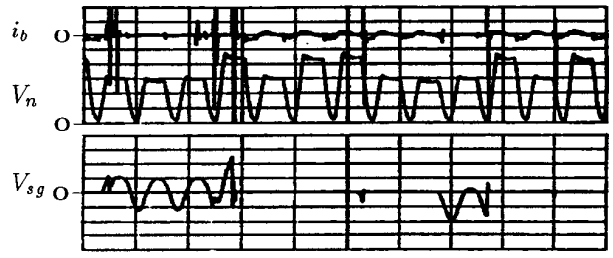

Fig. 17. Insulated-Real case with RDCL inverter; bearing current i_b [0.1 A/div] expanded scale, neutral voltage V_n [200 V/div], shaft voltage V_{sg} [20 V/div], $t = 20\mu s$/div

dc link inverter case shown in figure 21, the only bearing current that seems to flow is primarily due to the discharge mode. In this case the conduction mode duration is significantly longer compared to the case with one bearing real.

With both bearings shorted out to correspond to the *shorted-shorted* case, as shown in figures 22(a) and 22(b), there is seen to be high circulating current (0.5 – 1 A peak) in the bearings for both inverters. The PWM hard switched inverter currents had a sharper edge corresponding to the switching instants as shown in figure 22(a), compared to that with resonant dc link inverter as shown in figure 22(b). In this case, the circulating current was primarily high frequency, with little observable low frequency circulating component.

With one of the bearings made *real* (i.e. *real-shorted* case) as shown in figure 23, for soft switched resonant dc link inverter, the bearing current was observed to drop to very small levels. In contrast, for the PWM hard switched inverter case, significant current flow was observed, particularly at the inverter switching transients.

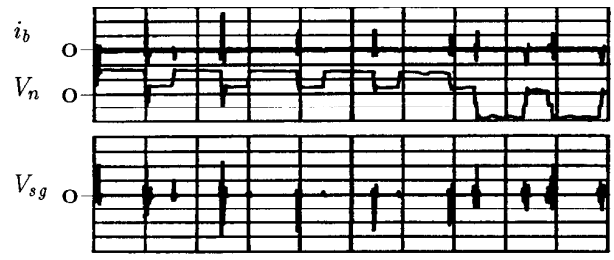

Fig. 18. Insulated-Shorted case with PWM inverter ; bearing current i_b [0.05 A/div], neutral voltage V_n [200 V/div], shaft voltage V_{sg} [1 V/div] expanded scale, $t = 100\mu s$/div

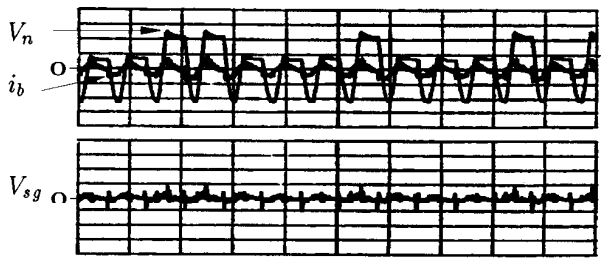

Fig. 19. Insulated-Shorted case with RDCL inverter ; neutral voltage V_n [200 V/div], bearing current i_b [0.1 A/div], shaft voltage V_{sg} [20 V/div], $t = 20\mu s$/div

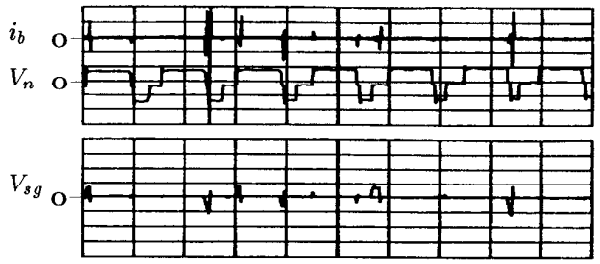

Fig. 20. Real Real case with PWM inverter ; bearing current i_b [1 A/div], neutral voltage V_n [200 V/div], shaft voltage V_{sg} [20 V/div], $t = 100\mu s$/div

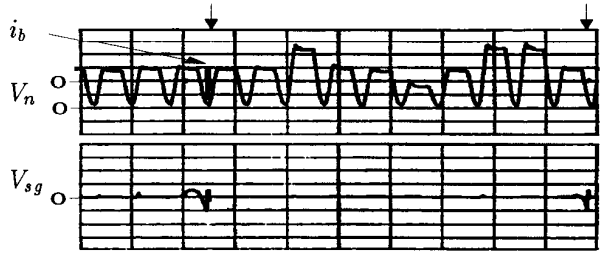

Fig. 21. Real-Real case with RDCL inverter ; bearing current i_b [0.1 A/div] expanded scale, neutral voltage V_n [200 V/div], shaft voltage V_{sg} [20 V/div], $t = 20\mu s$/div; arrows indicate bearing current spikes

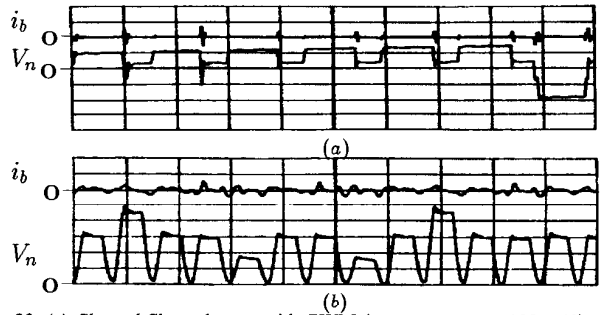

Fig. 22. (a) Shorted-Shorted case with PWM inverter, $t = 100\mu s$/div ; (b) Shorted-Shorted case with RDCL inverter, $t = 20\mu s$/div ; bearing current i_b [1 A/div], neutral voltage V_n [200 V/div]

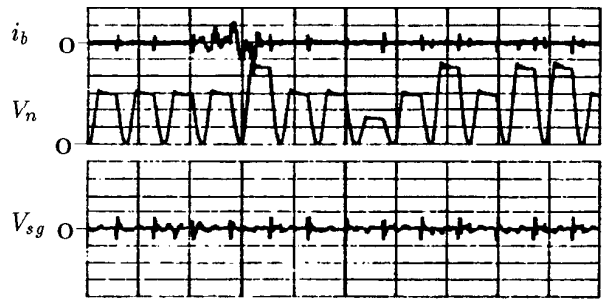

Fig. 23. Real - Shorted case with RDCL inverter ; bearing current i_b [0.05 A/div], neutral voltage V_n [200 V/div], shaft voltage V_{sg} [1 V/div] expanded scale, $t = 20\mu s/div$

VII. Conclusions

This paper perhaps raises more questions than it answers. Of particular significance are issues relating to the motor model. The development of a simple capacitive model of the machine, while accurate over a fairly broad range of frequencies, seems to be inadequate over the range of frequencies generated by PWM hard switching inverters. The model may actually be more accurate for zero voltage switched soft switched inverters, due to the limited band of frequencies generated on their output. The predominantly accepted hypothesis for bearing failures, i.e. solely EDM discharge currents, is questioned. It is felt that there may also be several contributing factors including smaller and more frequent dv/dt related current spikes, voltage sustaining capability of the lubricant film as a function of exciting frequency, and the possibility of circulating currents due to high frequency spatial asymmetries in the machine.

A small signal excitation test was conducted to monitor bearing behavior in a clean noise-free environment, and gave valuable insight into possible bearing current mechanisms. Finally operation with identical hard and soft switched inverters was compared.

The problem of bearing failure seems, in the authors' opinion, to be very complex. Contributing factors also include shaft and frame grounding locations, and voltages across bearings generated by capacitive currents flowing in the stator iron and shaft. It is also likely that low impedance grounds to motor case may increase common mode currents, and actually cause a higher driving point voltage. The high frequency flux induced by these ground currents flowing within the motor can also induce shaft voltages and circulating currents in shorted or low impedance bearings. This is being investigated and will be reported in a later paper.

One likely scenario suggests that bearing degradation occurs due to a combination of the various currents listed above. If one bearing degrades to the point where it tends to break down due to high dv/dt induced shaft voltage or EDM currents, then high circulating currents can flow, and bearing failure is greatly accelerated. Substantial work is required to unequivocally verify this hypothesis.

In general the authors feel that stronger evidence is required to support the observation that IGBT inverter driven motors have consistently higher field failure rates. The final analysis will have to take into account a detailed high frequency model of the machine, including winding asymmetries, distributed capacitances, stator iron impedances (particularly considering laminations), rotor impedances, connection to motor case, and ground impedances. The challenge is considerable as motor manufacturers presently pay no attention to motor behavior at frequencies of 10 kHz to 30 MHz, the frequency range of interest for analyzing response of motor bearings to hard switching inverters.

It is also too early to tell if soft switched inverters reduces bearing problems. However, lower dv/dt currents, and lower circulating currents with the *real-real* or *real-shorted* bearing cases, indicate the possibility for improved performance. Further investigations are on going, and will be reported in a future paper.

VIII. Acknowledgement

The authors wish to thank MagneTek and Marathon Electric Co. for providing the induction motors used for the experiments.

References

[1] P.F. Albrecht, et al., "Assesment of the Reliability of Motors in Utility Applications - Updated", IEEE Trans. on Energy Conversion, Vol. EC-1, No. 1, March 1986, pp 39-46.

[2] IAS Motor Reliability Working Group, "Report of Large Motor Reliability Survey of Industrial and Commercial Installations : Part I", IEEE Trans. on IA, Vol. IA-21, No. 4, July 1985, pp 853-864.

[3] P. Alger, H. Samson, "Shaft Currents in Electric Machines", Conf. of A.I.R.E., Feb., 1924.

[4] C. Ammann, K. Reichert, R. Joho, Z. Posedel, "Shaft Voltages in Generators with Static Excitation Systems - Problems and Solution", IEEE Trans. on Energy Conversion, Vol. EC-3, No. 2, June, 1988.

[5] R. Leimkuhler, "Bearing Fluting and Causes", Electrical Apparatus Service Association (EASA) Convention Presentation, 1996, Phoenix, AZ (available as audio-tape).

[6] P. Langhorst, C. Hancock, "Simple Truth about Motor Drive Compatibility", MagneTek Publication, 1996.

[7] J. Erdman, R.J. Kerkman, D. Schlegel, G. Skibinski, "Effect of PWM Inverters onAC Motor Bearing Currents and Shaft Voltages", IEEE-APEC Conf. Record, 1995, pp 24-33.

[8] D. Busse, J. Erdman, R.J. Kerkman, D. Schlegel, G. Skibinski, "Bearing Currents and Their Relationship to PWM Drives", IEEE Industrial Electronics Conf. Record, 1995, pp 698-705.

[9] D. Busse, J. Erdman, R.J. Kerkman, D. Schlegel, G. Skibinski, "The Effects of PWM Voltage Source Inverters on the Mechanical Performance of Rolling Bearings, IEEE-APEC Conf. Record, 1996, pp 561-569.

[10] D. Busse, J. Erdman, R.J. Kerkman, D. Schlegel, G. Skibinski, "System Electrical Parameters and Their Effects on Bearing Currents", IEEE-APEC Conf. Record, 1996, pp 570-578.

[11] A. Bonnett, "Analysis of AC Induction Motor Transients Caused by PWM Inverters", PQA'93/PECON IV Conf. Proceedings, Nov 1993, pp 4-3:1 - 4-3:14.

[12] A. Bonnett, "Analysis of the Impact of Pulse-Width Modulated Inverter Voltage Waveforms on AC Induction Motors", IEEE Trans. on IA, Vol. IA-32, No. 2, March/April 1996, pp 386-392.

[13] T.W. Atkins, "Voltage Ring-up Wear and Tear on Electric Motors by Inverters", Power Quality Assurance, Sept/Oct, 1995.

[14] S. Chen, T.A. Lipo, D. Fitzgerald, "Measurement and Analysis of Induction Motor Bearing Currents in PWM Inverter Drives", Proc. of Intl. Agean Conf. on Electrical Machines and Power Electronics, Turkey, 1995, pp 289-296.

[15] S. Chen, T.A. Lipo, D. Fitzgerald, "Modeling of Motor Bearing Currents in PWM Inverter Drives", IEEE-IAS Conf. Record, 1995, pp 388-393.

[16] Z. Krzemlen, "Voltages at Frame, Earth Currents and Bearing Currents Occurring in Induction Motors Fed from PWM Inverters - Measuring Results", Proc. of Intl. Agean Conf. on Electrical Machines and Power Electronics, Turkey, 1995, pp 283-288.

[17] D. Maly, "High-Frequency Time Harmonic Loss in Induction Motors" M.S. Thesis, University of Wisconsin-Madison, 1991.

[18] B.K. Gupta, D.K. Sharma, D.C. Bacvarov, "Measured Winding Impedances of a Large AC Motor", IEEE Trans. on Energy Conversion, Vol. EC-2, No. 1, March, 1987, pp 139-151.

[19] E.P. Dick, et al., "Prestriking Voltages Associated with Motor Breaker Closing", IEEE Trans. on Energy Conversion, Vol. EC-3, 1988, pp 855-861.

[20] D.M. Divan, "The Resonant DC Link Inverter A New Concept in Static Power Conversion", IEEE-IAS Conf. Record, 1986, pp 648-656.

[21] T.G. Habetler, D.M. Divan, "Performance Characterization of a New Discrete Pulse Modulated Current Regulator", IEEE-IAS Conf. Record, 1988, pp 395-405.